Cell

S. cerevisiae Chromosomes Biorient via Gradual Resolution of Syntely between S Phase and Anaphase

Eugenio Marco,[1,2,4,5] Jonas F. Dorn,[3,4] Pei-hsin Hsu,[1] Khuloud Jaqaman,[2,6] Peter K. Sorger,[2] and Gaudenz Danuser[1,*]
[1]Department of Cell Biology, Harvard Medical School, Boston, MA 02115, USA
[2]Department of Systems Biology, Harvard Medical School, Boston, MA 02115, USA
[3]Institute for Research in Immunology and Cancer, University of Montreal, Montreal QC H3C 3J7, Canada
[4]These authors contributed equally to this work
[5]Present address: Department of Biostatistics and Computational Biology, Dana-Farber Cancer Institute and Harvard School of Public Health, Boston, MA 02115, USA
[6]Present address: Department of Biophysics, UT Southwestern Medical Center, Dallas, TX 75390, USA
*Correspondence: gaudenz_danuser@hms.harvard.edu
http://dx.doi.org/10.1016/j.cell.2013.08.008

SUMMARY

Following DNA replication, eukaryotic cells must biorient all sister chromatids prior to cohesion cleavage at anaphase. In animal cells, sister chromatids gradually biorient during prometaphase, but current models of mitosis in *S. cerevisiae* assume that biorientation is established shortly after S phase. This assumption is based on the observation of a bilobed distribution of yeast kinetochores early in mitosis and suggests fundamental differences between yeast mitosis and mitosis in animal cells. By applying super-resolution imaging methods, we show that yeast and animal cells share the key property of gradual and stochastic chromosome biorientation. The characteristic bilobed distribution of yeast kinetochores, hitherto considered synonymous for biorientation, arises from kinetochores in mixed attachment states to microtubules, the length of which discriminates bioriented from syntelic attachments. Our results offer a revised view of mitotic progression in *S. cerevisiae* that augments the relevance of mechanistic information obtained in this powerful genetic system for mammalian mitosis.

INTRODUCTION

The elaborate dynamics of spindle assembly and checkpoint surveillance during mitosis have as their ultimate goal the proper attachment of replicated sister chromatids to kinetochore microtubules (kMTs) emanating from opposite spindle poles, a process referred to as chromosome biorientation. Failure to biorient chromatid pairs prior to dissolution of sister cohesion and mitotic exit causes aneuploidy, dramatically lowering the viability of single-cell organisms and promoting cancer and birth defects in mammals (Chandhok and Pellman, 2009; Draviam et al., 2004; Thompson et al., 2010). Understanding mitosis ultimately comes down to understanding mechanisms that promote efficient biorientation and couple cell-cycle progression to acquisition of this geometry by all chromosomes.

Because of its powerful genetics and relatively simple spindle and kinetochores, the budding yeast *S. cerevisiae* is a good organism in which to study spindle assembly and mitotic progression. Prevailing models suggest that biorientation is established in budding yeast at the earliest stages of spindle assembly (Goshima and Yanagida, 2000). Subsequently, poleward forces exerted by kinetochore-bound microtubules pull apart the 16 sets of sister kinetochores and their associated pericentric DNA (Yeh et al., 2008). Chromosomes are postulated to remain in this bioriented configuration until the onset of anaphase (Gardner et al., 2005, 2008; Pearson et al., 2004), at which point cohesion between sisters is lost, allowing the two sets of sisters to separate and move toward the spindle poles. A key argument in favor of this model is that virtually all kinetochore proteins (typically visualized as GFP fusions) localize from the onset of mitosis until anaphase into two distinct lobes that lie along the spindle axis. Such a stable bilobed distribution is assumed to be synonymous with chromosome biorientation (Goshima and Yanagida, 2000; He et al., 2000; Hyland et al., 1999; Pearson et al., 2001; Zeng et al., 1999) and is consistent with electron micrographs showing that the mitotic spindle consists of ~16 short microtubules (MTs) emanating from each spindle pole body (SPB) and two sets of four interpolar MTs that interdigitate to form a connection between the poles (O'Toole et al., 1999; Winey et al., 1995). The short MTs are assumed to be bound to bioriented and separated kinetochores.

One unappealing aspect of budding yeast as a model for chromosome segregation is that it seems very different from what is observed in many other eukaryotes, including humans, in which bipolarity is established gradually over the course of a relatively long prometaphase (Kitagawa and Hieter, 2001). However, none of the studies on budding yeast actually rule out the possibility that the two bilobes contain a mixture of bioriented and syntelic kinetochores. Observing the consequential gradual resolution of

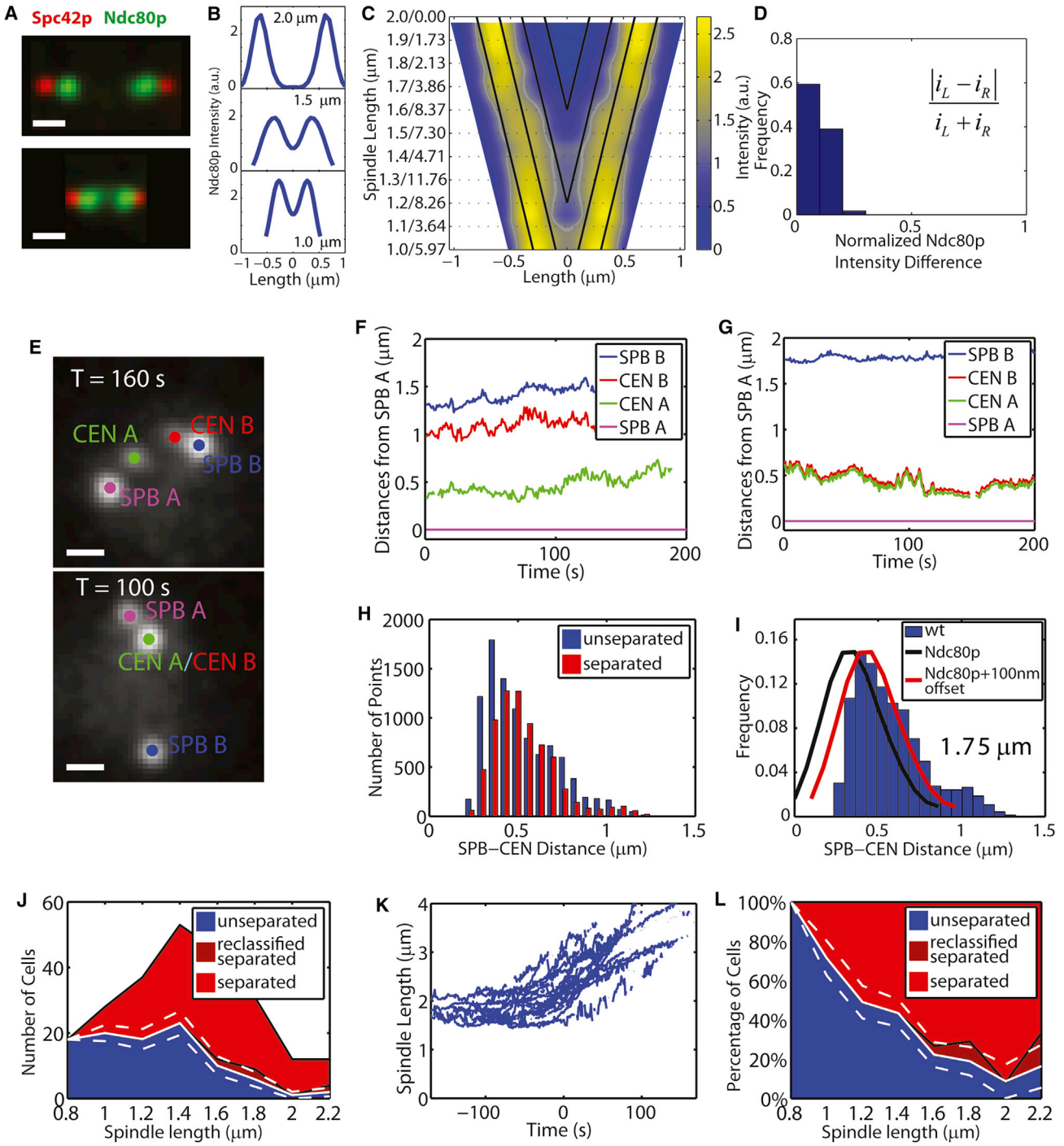

Figure 1. WT Cells Show Bilobed Distribution of Kinetochores in Metaphase but Establish Bipolarity Only Gradually

(A) Representative intensity projections of 3D image stacks of fixed WT cells coexpressing Spc42-CFP (red) marking SPBs and Ndc80-GFP (green) marking kinetochores. Scale bar, 0.5 μm.

(B and C) Symmetrized Ndc80p distributions of n = 59 cells. Cells were ranked according to spindle lengths, which varied between 1 μm (bottom) and 2 μm (top) in (B). V plots show combined Ndc80-GFP intensity profiles as a function of spindle length (see Experimental Procedures). The SPB is located at the boundary of the trapezoidal intensity map. Diagonal black lines indicate loci of constant distance to the SPBs in steps of 0.2 μm.

(D) Distribution of the relative intensity difference between Ndc80p bilobes (see Experimental Procedures).

(E) Representative maximum intensity projections of CEN IV and SPB tags in cells with separated (top) and unseparated (bottom) sisters. Scale bar, 0.5 μm.

(F and G) Time courses of distances between SPB A and SPB B (blue) and between SPB A and proximal (CEN A, green) and distal (CEN B, red) CEN IV tag. The cell in (F) has a spindle length of ~1.4 μm with separated CEN IV tags. The cell in (G) has a spindle length of ~1.75 μm with still-unseparated CEN IV tags.

(legend continued on next page)

syntelic attachments is expected to be difficult; rapid rates of MT growth and shrinkage (up to ~4 μm/min) (Dorn et al., 2005) combined with the small size of the yeast spindle (~1.5 μm) imply that the movement of a kinetochore from one lobe to the other would take only 10–20 s. Following such an event, the intensity of the two kinetochore lobes is expected to change by at most 10%, also making it difficult to detect the kinetochore rearrangement. Nonetheless, transient separation of sister centromeres and subsequent movement of kinetochores across the spindle midzone has been detected (He et al., 2000).

This paper attempts to distinguish directly between the early-biorientation model for yeast and a more evolutionarily plausible progressive-biorientation model accepted for higher eukaryotic cells. We combine various tagging and single-chromosome imaging strategies with statistical analysis of large numbers of wild-type (WT) and mutant yeast cells to provide evidence that, like human kinetochores, yeast kinetochores progressively biorient over the entire period from S phase to anaphase onset.

RESULTS

Three Assays to Track Kinetochore Attachment and Organization

We developed three assays to investigate the establishment of biorientation during yeast mitosis, each illuminating a different facet of the process. (1) The kinetochore-snapshot assay involves acquisition of three-dimensional (3D) images of an unsynchronized population of fixed cells using a fluorescently tagged kinetochore (Ndc80-GFP) and spindle pole body (Spc42-CFP) protein. The distance between spindle poles serves as a proxy for mitotic progression because spindle length increases monotonically from early S phase to anaphase onset, making it possible to follow the distribution of all 16 kinetochore pairs at successive stages of mitosis (Figures 1A–1D and Figure S1A available online), albeit with no information on individual kinetochores. (2) The CEN IV-tracking assay involves 3D time-lapse imaging and machine-vision-assisted tracking of fluorescent spots marking the motion of the centromere-proximal region of chromosome IV (CEN IV; tagged using a Tet-Operator insert and a Tet-Repressor fused to GFP) relative to the SPBs (labeled with Spc42-GFP). Such dynamic data provide a more direct view of sister chromatid attachment at different stages of mitosis and have the benefit of rapid temporal sampling (1 Hz; Figures 1E–1G) but only during a short period of time (photobleaching limits the movies to ~200–300 s duration) and for a single kinetochore. (3) The CEN IV-snapshot assay involves imaging the position of CEN IV-proximal GFP tags at a single point in time but for many cells simultaneously. This assay is complementary to the CEN IV-tracking assay in that it determines the position of CEN IV tags relative to SPBs in hundreds of cells. Using the separation of CEN IV tags as a marker for bipolar attachment and assuming that chromosome IV is representative of all chromosomes, we extrapolated on a statistical basis the relationship between biorientation and mitotic progression for the entire ensemble of chromosomes.

Kinetochore Distribution Is Bilobed and Symmetric for Spindles Longer Than One Micrometer

We used the kinetochore-snapshot assay to monitor successive changes in mean kinetochore distribution as a function of SPB-SPB distance and, thus, as a function of position in mitosis (Figures 1A–1C and Movie S1). We found that the intensity distribution was bilobed for spindles longer than ~1.1 μm (n = 59 cells) and that the peaks of the two lobes were on average ~0.35 μm away from the spindle poles (Figure 1C). As the spindle length increased over the course of mitosis, the kMT length stayed constant, and the distance between the kinetochore lobes increased.

Soon after START, budding yeast SPBs undergo a semiconservative process of replication, giving rise to distinct new and old SPBs (Jaspersen and Winey, 2004). Yeast kinetochores are known to preferentially attach to the old SPB early in mitosis (Maure et al., 2007; Tanaka et al., 2002), and we therefore asked whether such preferential attachment resulted in a difference in the peak intensities of the two lobes. We used the kinetochore-snapshot assay to observe the distribution of all kinetochores via Ndc80-GFP. For each individual cell, we calculated the asymmetry score $|i_L - i_R|/(i_L + i_R)$, where i_L and i_R are the total Ndc80-GFP intensities on the left and right of the spindle midzone, respectively (Figure 1D). For all spindle lengths, we observed a tight distribution of scores around 0, showing that similar numbers of kinetochores were present in each lobe (Figures 1D and S1B). This suggests that, even though kinetochores may initially prefer to attach to the old SPB, a mechanism must exist for symmetrizing the distribution, potentially via detachment and reattachment prior to significant SPB separation.

The Bilobed Distribution of Kinetochores Results from a Tight Regulation of SPB-CEN Distance, Regardless of the Type of Attachment

Although bioriented attachment of chromosomes to microtubules is expected to result in a bilobed and symmetric

(H) Histograms of SPB-CEN distances in cells with unseparated tags (blue) and separated tags (red). For cells with unseparated tags, only the overall shortest SPB-CEN distance is included.

(I) Normalized histogram of SPB-CEN distances from cells with spindle lengths between 1.5 and 2 μm. Black line, Ndc80p intensity distribution in an average spindle with a length of 1.75 μm (derived from the V plot in C). Red line, Ndc80p intensity distribution shifted by 100 nm, indicating the offset between Ndc80p and CEN IV tags.

(J) Distribution of spindle lengths in CEN IV-snapshot assay and classification into unseparated (blue), separated (light red), and reclassified as separated (dark red) CEN IV tags. White solid and dashed lines indicate mean ± bootstrapped SD of cells with syntely. See Experimental Procedures and Figure S2 for details.

(K) Time courses of SPB A-SPB B distances for cells entering anaphase. The time courses are aligned relative to one another with T = 0 s representing the frame in which the two chromosome tags start recoiling.

(L) Normalized distribution of unseparated (blue), separated (light red), and reclassified as separated (dark red) CEN IV tag as a function of spindle length (derived from J). White lines indicate mean ± bootstrapped SD of cells with syntely.

See also Figures S1, S2, and S3, Tables S1 and S2, and Movies S1, S2, S3, and S4.

distribution of kinetochore proteins, alternative configurations involving mixtures of syntelic, monotelic, and bioriented sisters would also give rise to a bilobed pattern (Figures S1C–S1E). To investigate the actual state of kinetochore, we turned to the CEN IV-tracking assay. In the tracking assay, biorientation results in separation of the two CEN tags, and this separation can be resolved visually down to the diffraction limit of the imaging system (~250 nm) (He et al., 2000; Pearson et al., 2001) (Figure 1E, top). Replicated sisters attached in monotelic or syntelic configurations lack the tension required for centromere tag separation, and the two CEN IV tags appear as one unresolved spot (Figure 1E, bottom). We imaged cells for 200–300 s, acquiring z stacks of 16 slices separated by 200 nm every second, and used computational procedures to track tags in 3D with a localization precision of ~20 nm (Movie S2) (Thomann et al., 2002, 2003). Our tracking software achieves a super-resolution improvement of ~2-fold (relative to the diffraction limit), allowing two CEN IV tags to be resolved to distances of $\geq$150 nm (Dorn et al., 2005) (Supplemental Information).

We observed CEN IV tags with separated (Figure 1F) and unseparated (Figure 1G) CEN IV kinetochores in cells having either short or long spindles, suggesting that bipolar attachments could be established at different points in mitotic progression. We also observed CEN IV tags transitioning from unseparated to separated (Movie S3). SPB-CEN IV distances remained approximately constant throughout mitotic progression, with no major difference in presumed kMT length between separated (n = 20 cells) and unseparated (n = 27 cells) tags (Figure 1H). The distribution of SPB-CEN IV distances (for spindle lengths between 1.5 and 2 μm) was very similar to the Ndc80-GFP intensity distribution as established in the kinetochore-snapshot assay but with the peak shifted ~100 nm toward larger distances (Figure 1I). This arises from a 50–90 nm positional offset between the GFP tag on the C terminus of Ndc80 and the center of the Tet-GFP operator array (Dorn et al., 2005; Joglekar et al., 2009), as well as from the apparent reduction in Spb42-CFP to Ndc80-GFP distance when projected on the SPB-SPB axis. These observations imply that one important contributor to the bilobed distribution of kinetochore proteins is the tight regulation of SPB-CEN distances for chromatids, regardless of their monopolar or bipolar attachment.

Live-cell tracking of CEN IV tags occasionally showed frames with "hyper-stretched" tags (Figure S1F), where the pericentric DNA of the chromatid attached to the closer SPB remained compacted, whereas the pericentric DNA of the sister chromatid attached to the more distant pole unraveled under tension. Such asymmetric stretching is consistent with a model in which both chromatids can have unseparated arms in the same lobe while a microtubule from the distant pole pulls one of the two kinetochores into the opposite lobe. The model implies that cohesion remains intact along the arms of sisters that are sterically trapped in one spindle half while the pulling force from the microtubule of the distant pole is sufficient to unravel the pericentric chromatin of one sister (Yeh et al., 2008).

Together, these CEN IV-tracking data showed that the establishment of bipolarity occurred at random times during mitotic progression and that some cells did not establish biorientation of CEN IV until late in mitosis. However, our 47 live-cell movies were acquired with the goal of obtaining an almost equal number of cells with separated and unseparated tags (Figures S2A and S2B). Analysis of individual frames showed that separated tags were likely to be underrepresented (Figures S2C and S2D). Therefore, we turned to the CEN IV-snapshot assay for an unbiased sampling of the extent of chromatid separation.

Biorientation Is Established Gradually up to Anaphase Onset

We imaged CEN IV tags relative to SPBs in an asynchronous population of n = 828 cells (see Table S1 and Figures S2E–S2H). Because the sampling was random with respect to the cell cycle, the frequency of occurrence of a particular spindle length was inversely proportional to the rate of spindle elongation at this length. The observed peak in the spindle length at ~1.4 μm arises because spindle elongation slowed down at this stage of mitosis (Figure 1J). Beyond this length, the distribution monotonically decreased until the spindle length was ~2 μm, at which point cells entered anaphase (Figure 1K and Movie S2). The fraction of spindles having separated CEN IV tags provided a direct measure of the probability of biorientation throughout mitosis (Figure 1L). Our analysis explicitly accounted for the possibility that spindles, in which only one CEN IV spot was detected, represented configurations with bioriented attachment but that the signal arising from one tag was undetectable either because of hyperstretching or because the CEN IV tag was unresolvable from the SPB (Figure 1L, dark red, and Figure S2; Supplemental Information). Using these approaches, we estimated that, for spindle lengths ~1–1.2 μm, ~50% of the CEN IV tags were bioriented, and this percentage increased to ~80% at 1.6 μm. Cells reached a state of complete bipolarity only at ~2 μm, shortly before anaphase onset.

The quasiexponential decay of the fraction of separated tags would be consistent with the notion that bipolarity is established in a random process throughout mitosis. Nonetheless, we were concerned that the CEN IV-snapshot assay could lead to an underestimation of the fraction of sisters with separated tags because of the asymmetric location of the 11 kb TetO-array on one of the chromosome arms (Figure S3A). It is conceivable that sister kinetochores separate by unraveling pericentric DNA without breaking down cohesion in the region of the array insert. To address this issue, we repeated our measurements in a strain in which the tag involved symmetric insertion of two short ~6 kb TetO repeats −360 bp and +370 bp from CEN IV (Figure S3A). The resulting spot signal displayed a compact, subresolution distribution of TetR-GFPs (Movie S4), which we verified by comparing the residuals of fitting the spot with a 3D point spread function (PSF) to background noise (Thomann et al., 2002). Contrary to the previously used 11 kb TetO-array, the centroids of each of these symmetric TetO-arrays are located at 3.4 kb, which is outside the cohesive part of bioriented chromosome arms (estimated to start at 4 kb [Pearson et al., 2001]). Accordingly, more than half (~60%) of the arrays locate in the pericentric chromatin region that follows the separating kinetochore but occasionally may also be stretched out in a bipolar attachment. Therefore, although it is still possible with the symmetric tag design that bioriented sisters generate a single fusion spot of both tags, the probability of unresolved tag separation

during biorientation is much lower, especially for longer spindles shortly before anaphase, and the fusion spot will not have the properties of a diffraction-limited signal (Figure S3B). Stretched fusion spots were identified by the PSF fitting procedure either as a signal mixture of two separated, bioriented tags or as unclassifiable (Supplemental Information). Application of our super-resolution CEN IV-tracking assay to the symmetric tag strain confirmed with high confidence that cells with unseparated CEN IV tags were present at long spindle lengths and that, in this case, the tag intensity was higher than in cells with separated tags (n = 94, Figures S3C–S3F). We also reproduced the finding from the CEN IV-snapshot assay using the symmetric tag strain that bona fide unseparated tags and thus mono-orientation existed until anaphase onset (n = 3,817 cells, out of which 925 were in mitosis, see Table S1 and Figures S3G and S3H).

Taken together, these experiments demonstrate that biorientation occurs gradually in budding yeast during a period of prometaphase that is 20–25 min in duration, followed by a much shorter metaphase—if any—in which biorientation is complete but anaphase has not yet begun; anaphase ensues soon after that last sister chromatid is bioriented. Interestingly, the proposed ~25 min duration of prometaphase in *S. cerevisiae* is similar to that of prometaphase in mammalian cells but includes the majority of the ~30 min length of yeast mitosis, whereas in mammalian cells, prometaphase covers only a fraction of the 120 min of mitosis. This suggests that mechanisms of biorientation during prometaphase are conserved between yeast and mammalian cells, whereas the roles of metaphase may differ.

Syntelic Attachments in *ipl1-321* Mutant Cells Have Tightly Constrained SPB-CEN Distances

Our hypothesis that a bilobed kinetochore distribution can arise from roughly equal partitioning of sister chromatids having syntelic attachment to the two SPBs demands that the SPB-CEN distance of syntelic attachments be tightly regulated. To determine whether this is true, we examined mutants of Ipl1p, a key player in the resolution of syntelic attachment (Biggins et al., 1999; Tanaka et al., 2002). In *ipl1-321* cells, which carry a temperature-sensitive loss-of-function mutation (Biggins et al., 1999), failure to resolve syntely at the restrictive temperature (37°C) leads to asymmetric chromosome segregation in 70%–85% of cells (Biggins et al., 1999; Kim et al., 1999; Pinsky et al., 2003; Tanaka et al., 2002). Consistent with this, when we applied the kinetochore-snapshot assay to *ipl1-321* cells, we observed kinetochore distributions that were much more asymmetric than in WT cells (Figures 2A and 2B). CEN IV tracking showed that the majority of sisters had unseparated tags (Figure 2C and Movie S5) with an SPB-CEN IV distance of 0.53 ± 0.07 μm (Table S2).

CEN IV-snapshot assays of asynchronous *ipl1-321* cell populations revealed a very different distribution of spindle lengths as compared to WT cells (Figure 2D). Whereas spindle length peaked at ~1.4 μm in WT cells, it peaked at 2.0–2.5 μm in *ipl1-321* cells and fell monotonically to a maximum SPB-SPB distance of 3 μm, a length at which WT cells are well into anaphase. The differences in elongation dynamics may be related to aberrant operation of the spindle checkpoint (Pinsky and Biggins, 2005) or rapid progress to 2 μm length followed by a delay for recruitment of factors required for anaphase onset. Regardless, by anaphase onset in *ipl1-321* cells, we observed that only ~30% of the initially monopolar attachments had been resolved into bipolar attachments (Figure 2E).

Despite their predominant syntely (Tanaka et al., 2002), the SPB-CEN IV distance of *ipl1-321* cells was tightly regulated, as evidenced by a sharp peak in the length distribution at 0.5 μm (Figure 2C). Remarkably, the position centers of unseparated and separated CEN IV tags perfectly colocalized with the position centers of unseparated and separated tags in WT cells at 37°C (Table S2; the difference in SPB-CEN distance between room temperature and 37°C arises from differences in microtubule dynamics at elevated temperatures [Dorn et al., 2005; Jaqaman et al., 2006]). This provides evidence that the bilobed intensity distribution results from the tight regulation of SPB-CEN distances rather than from sister chromatid separation due to biorientation.

stu2-277 Mutant Cells Fail to Establish Bipolar Attachments yet Exhibit a Bilobed Kinetochore Distribution

An alternative way to probe the connection between bipolarity and bilobed kinetochore distributions is to examine mutations in which defects in kMT dynamics interfere with kinetochore-microtubule capture. We studied this in cells carrying a mutation in the microtubule-associated protein XMAP215/Stu2p (Brouhard et al., 2008; Vasquez et al., 1994; Wang and Huffaker, 1997). Although *stu2-279* or *stu2-277* cells establish bilobed kinetochore distributions at the restrictive temperature (Gillett et al., 2004), they arrest in a checkpoint-dependent fashion (He et al., 2001; Severin et al., 2001), which arises from a defect in kMT dynamics (Pearson et al., 2003). We confirmed that *stu2-277* cells at 37°C exhibited bilobed kinetochore distributions (Figure 3A). Regardless of point in mitosis, kinetochore lobes were ~0.4 μm from the SPBs (Figure 3B). Analysis of 55 cells showed that *stu2-277* cells often had kinetochore lobes that spread perpendicular to the spindle axis (Figure 3A) and that were less symmetric across the spindle midzone than those in WT cells (Figure 3C) although more symmetric than in *ipl1-321* cells. CEN IV tracking in live cells (Movie S6) showed that, in *stu2-277* cells, the SPB-CEN IV distance was tightly controlled with a mean value of 0.51 ± 0.06 μm (a value similar to WT and *ipl1-321* cells; Figure 3D and Table S2). The majority of cells (38 of 50) had unseparated tags (Figure 3E), suggesting that, in *stu2-277* cells, a nearly symmetric bilobed distribution of kinetochores can arise early in mitosis even in the absence of sister separation and bipolarity. A minority of cells (6 of 50) contained separated CEN IV tags (Movie S6), and a further set of 6 cells contained CEN IV tags that lay well away from the spindle axis in a position that is characteristic of detached chromosomes (Movie S6). Consistent with our data on WT and *ipl1-321* cells, the SPB-CEN IV distance distributions for unseparated and separated tags in *stu2-277* cells strongly overlapped (Figure 3D), supporting the notion that each of the two lobes of Ndc80-GFP intensity contains a mixture of mono- and bioriented kinetochores.

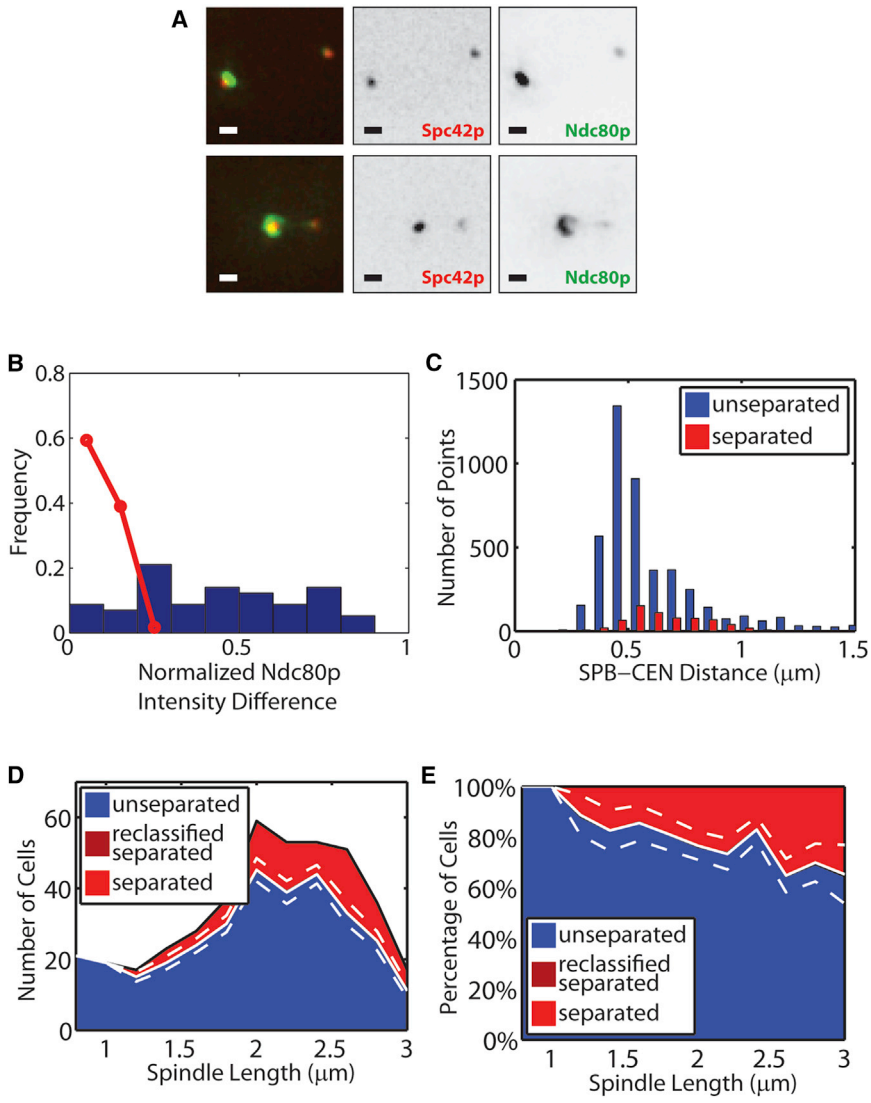

Figure 2. *ipl1-321* Cells Show Asymmetric Kinetochore Distributions but Have Tightly Regulated Kinetochore-Microtubule Lengths

(A) Representative intensity images (analogous to Figure 1A) of Spc42p and Ndc80p in *ipl1-321* cells. Scale bar, 0.5 μm.

(B) Distribution of the relative intensity difference between Ndc80p bilobes (analogous to Figure 1D for WT cells). Data are from n = 58 cells. Red line, distribution in WT cells.

(C) Histograms of SPB-CEN distances in cells with unseparated tags (blue) and separated tags (red) (analogous to Figure 1H for WT cells).

(D and E) Raw (D) and normalized (E) distributions of spindle lengths and classification into unseparated (blue) and separated (light red) CEN IV tags; *ipl1-321* cells do not contain spindles with reclassified CEN IV tags. White solid and dashed lines indicate mean ± bootstrapped SD of syntely (see Figures 1J and 1L).

See also Tables S1 and S2 and Movie S5.

The CEN IV-snapshot assay of asynchronous *stu2-277* cell populations showed that spindle elongation slows at ~1.2 μm length (Figure 3E). Compared to WT, the peak is narrower and higher, suggesting that *stu2-277* cells spend more time at this stage of mitosis. About 90% of the spindles had unseparated tags throughout mitosis (Figure 3F and Table S1), confirming that, in these cells, the Ndc80-GFP bilobes consist primarily of mono-oriented kinetochores.

To further elucidate the impact that functional impairment of a MT-associated protein can have on spindle organization, we analyzed the tubulin distribution along the SPB-SPB axis (Figure S4). Both WT and *stu2-277* cells showed intensity maxima 0.25–0.35 μm from the SPBs for all spindle lengths, which is consistent with a model in which most spindle microtubules correspond to kMTs ending at the kinetochore bilobes, whereas a few interpolar microtubules cross the spindle midzone and stretch between the poles. In WT cells, tubulin intensity maxima colocalized with the kinetochore lobes and were about twice as high as the midzone intensity for spindles in the length range 1.1–1.9 μm. This is consistent with the idea that each lobe is associated with 16 kMTs and the midzone with 8 microtubules. In contrast, *stu2-277* cells had a maxima-to-midzone intensity ratio of ~1.25 for spindles up to 1.6 μm in length, suggesting that only ~10 kMTs end in each of the bilobes. Together with our finding that most kinetochores in one lobe belonged to unseparated sisters with a monopolar attachment, this implies that the majority of these attachments are monotelic. Thus, although defects in *STU2* function have little effect on the length regulation of kMTs, they may prevent MTs from growing to a length where they can reach from one SPB across the midzone to capture kinetochores in a distant lobe. Consequently, correction of syntely is dramatically impaired.

cin8Δ Mutant Cells Exhibit a Weaker Bilobed Distribution of Kinetochores due to Less-Regulated SPB-CEN Distance

Our data thus far suggest that the bilobed distribution of kinetochores is the result of tight kMT length regulation, regardless of whether sister chromatids have achieved bipolar attachment. To test the consequences of disrupting this regulation, we deleted the kinesin-5 motor protein Cin8p, which has been shown to control kMT length (Gardner et al., 2008) and the processes that shape the bilobed kinetochore distribution (Gardner et al., 2008; Tytell and Sorger, 2006).

Consistent with previous reports, our assay revealed a looser and less clearly defined kinetochore distribution in *cin8Δ* than in WT cells (Figures 4A–4C; n = 104 cells), although a bilobed

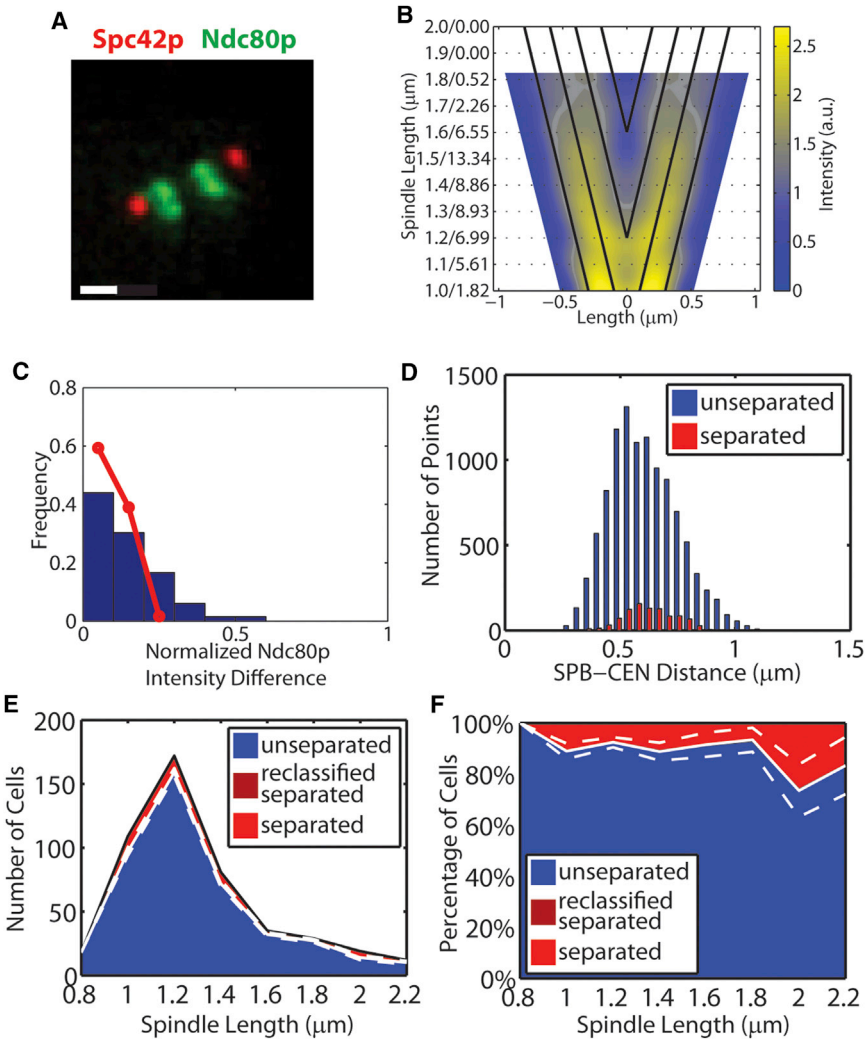

Figure 3. *stu2-277* Cells Show Symmetric Kinetochore Distributions and Have Regulated Kinetochore-Microtubule Length but Establish Few Bipolar Attachments

(A) Representative intensity images (analogous to Figure 1A) of Spc42p and Ndc80p in *stu2-277* cells. Scale bar, 0.5 μm.

(B) Symmetrized Ndc80p distributions of n = 55 *stu2-277* cells (analogous to Figure 1C for WT cells).

(C) Distribution of the relative intensity difference between Ndc80p bilobes (analogous to Figure 1D for WT cells). Red line, distribution in WT cells.

(D) Histograms of SPB-CEN distances in cells with unseparated tags (blue) and separated tags (red) (analogous to Figure 1H for WT cells).

(E and F) Raw (E) and normalized (F) distributions of spindle lengths and classification into unseparated (blue) and separated (light red) CEN IV tags; cells do not contain spindles with reclassified CEN IV tags. White solid and dashed lines indicate mean ± bootstrapped SD of cells with syntely (see Figures 1J and 1L).

See also Figure S4, Tables S1 and S2, and Movie S6.

distribution was visible in some cells (Figure 4A) with Ndc80-GFP intensity peaking ~0.30 μm from the SPBs (Figure 4B). The maxima were less well-defined than in WT cells, especially for spindles with a length close to ~2.0 μm (Figure 4C). However, *cin8Δ* cells had nearly equal numbers of kinetochores attached to each SPB (Figure 4D). In agreement with these data, live-cell trajectories displayed increased fluctuations in the SPB-CEN IV distances in *cin8Δ* cells (n = 25 cells) (Figures 4E–4G) and higher growth and shrinkage speeds than in WT cells (Table S2). The larger CEN IV tag displacements in *cin8Δ* cells were accompanied by frequent spindle midzone crossings (60% in *cin8Δ* cells compared to 11% in WT; Figures 4E and 4F, Movie S7, and Table S2) and resulted in a longer tail in the SPB-CEN IV distance distribution (Figure 4H). We also observed more transient separation and rejoining of CEN IV tags before anaphase (Figure 4G and Movie S7). A substantial portion of the tags remained unseparated until anaphase in *cin8Δ* cells (Figures 4I and 4J). Because *cin8Δ* cells have a low rate of chromosome loss (Hoyt et al., 1992), it cannot be that all sister chromatids with unseparated tags have monotelic or syntelic attachments. Instead, in the absence of Cin8p, tension across chromatids with bipolar attachments is reduced, and the length of kMTs is aberrant. The presence of tensionless bipolar attachments implies that kinetochore sisters in the same lobe have one long kMT emanating from the opposite SPB. In agreement with this, the tubulin distribution revealed higher intensities in the spindle midzone (Figure S4C).

DISCUSSION

In this paper, we provide evidence that biorientation of *S. cerevisiae* chromosomes is achieved gradually over an extended period of the cell cycle from S phase to anaphase onset and thus that the fundamental features of progressive biorientation are conserved between yeast and man. Pairs of sister kinetochores enter *S. cerevisiae* mitosis with a syntelic rather than a monopolar orientation as in mammalian cells, but in both cases, we propose that biorientation requires kinetochore-microtubule capture, the imposition of pulling forces, and separation of centromere-proximal, but not distal, chromatin. These findings augment the relevance of mechanistic information obtained from yeast, which offers powerful genetics and a much simpler spindle geometry for the analysis of the molecular regulation of mitotic processes.

We arrived at this alternate model of yeast mitosis by combining live-cell tracking of single kinetochore pairs with unbiased statistical assays of single kinetochore localization and kinetochore population distributions in large numbers of WT and *ipl1-321*, *stu2-277*, and *cin8Δ* mutant cells. Our model implies that the characteristic bilobed distribution of kinetochore proteins visible throughout mitosis does not arise from two sets of separated sister chromatids as commonly assumed; instead,

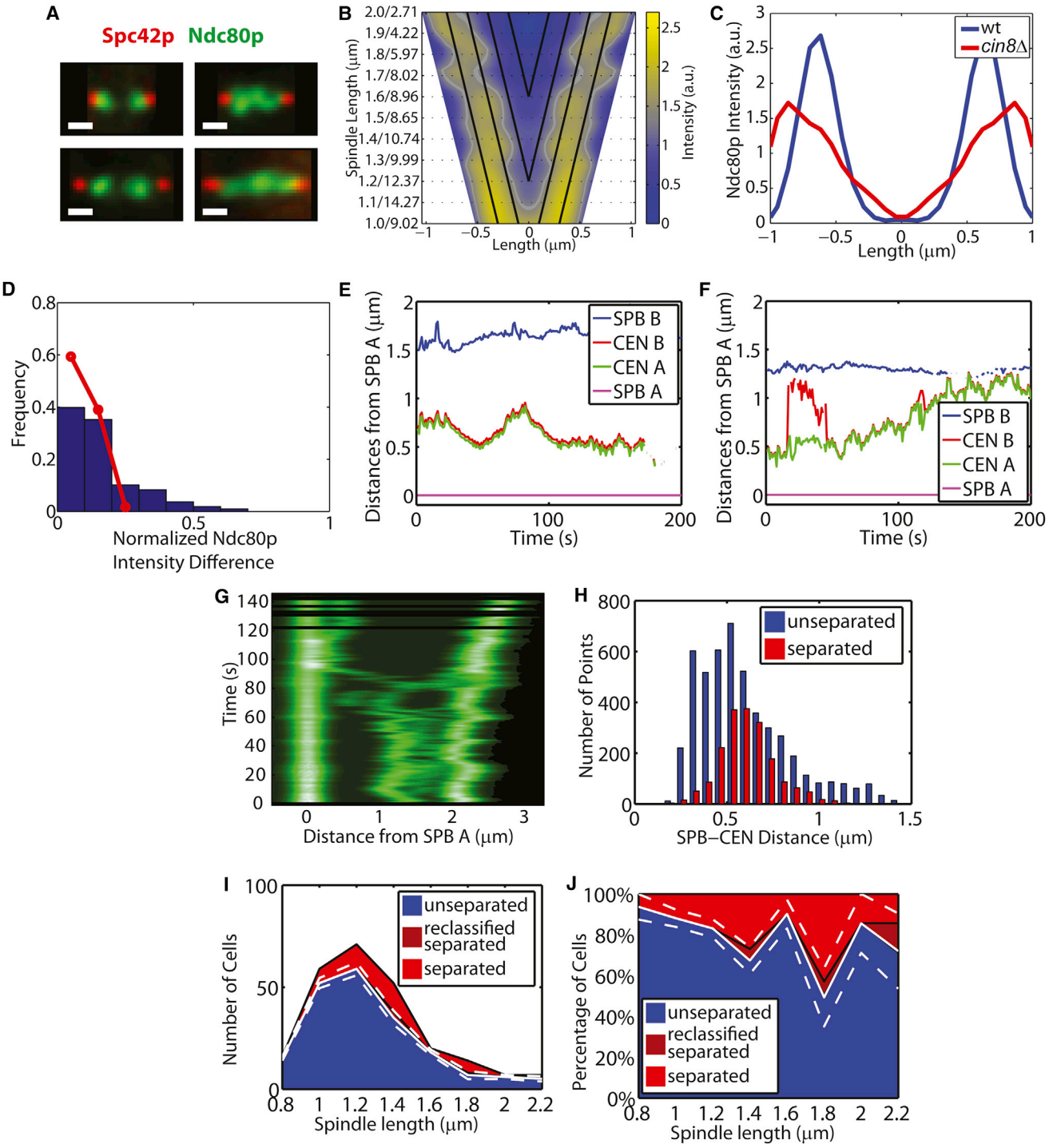

Figure 4. *cin8Δ* Cells Show Symmetric Kinetochore Distributions and Have Less-Regulated Kinetochore-Microtubule Lengths, Leading to Transient Fusion of Bioriented Sister Kinetochores

(A) Representative intensity images (analogous to Figure 1A) of Spc42p and Ndc80p in *cin8Δ* cells. Scale bar, 0.5 μm.

(B) Symmetrized Ndc80p distributions of n = 104 *cin8Δ* cells (analogous to Figure 1C for WT cells).

(C) Comparison of the WT (blue) and *cin8Δ* (red) Ndc80p distributions at 2 μm spindle length.

(D) Distribution of the relative intensity difference between Ndc80p bilobes (analogous to Figure 1D for WT cells). Red line, distribution in WT cells.

(E and F) Time courses of distances from SPB A to other tags (analogous to Figure 1F) for two cells with spindle midzone crossings by CEN IV tags. The example (F) shows a cell with transient separation and fusion of sister CEN IV tags, suggesting that the sisters have established biorientation but that the kinetochore-microtubule length is deregulated.

(legend continued on next page)

each lobe contains a mixture of bioriented and syntelic pairs until just prior to anaphase, at which point all pairs achieve biorientation.

We also find that the conserved feature of the bilobed kinetochore geometry is not the distance between the lobes (which increases over the course of mitosis) but rather the distance between each lobe and the spindle pole it is associated with, which remains constant at ~300–400 nm from S phase to anaphase. Our data suggest that this arises from tight regulation of the length of kMTs. We have previously shown that, in G1, SPB−CEN distances also measure ~400 nm (Dorn et al., 2005), implying that kMT length may be controlled by a universal mechanism that is independent of the cell-cycle phase and the geometry of chromosome-MT attachment. Recent studies in vivo and in vitro have identified the kinesins Cin8p and Kip3p as plausible candidates for length-sensitive regulators of kMT dynamics (Gardner et al., 2008; Su et al., 2011; Varga et al., 2009), and our experiments with *cin8Δ* mutants indeed show that the maintenance of the characteristic kinetochore bilobes requires correct regulation of kMT dynamics at a set length of 300–400 nm.

Implications for the Role of Ipl1/Aurora B in Yeast Mitosis

The prevailing model in which yeast kinetochores biorient early in mitosis poses several puzzles. (1) If all kinetochores are bioriented immediately after S phase, why does it take ~90 min until anaphase onset? (2) What, if not monitoring a gradual biorientation, is the function of the many components of the spindle assembly checkpoint that are conserved between yeast and man? (3) Why are kinetochore proteins and pathways that serve the resolution of syntely in mammalian cells highly conserved in yeast? This applies in particular to the Ipl1/Aurora B kinase, which, in mammalian cells, phosphorylates components of tension-free sister kinetochores to promote release of erroneous microtubule attachments (Cimini et al., 2006; Knowlton et al., 2006). Loss-of-function mutants of Ipl1p dramatically increase aneuploidy in *S. cerevisiae* (Chan and Botstein, 1993) and prevent meiosis progression (Meyer et al., 2013), suggesting that error correction is required also in yeast to ensure proper segregation of sister chromatids. Whether the function of *IPL1* is restricted to only the earliest moments of mitosis as implied by the early-biorientation model or is essential throughout had yet to be determined.

No tension can be exerted on bipolar attachments until the spindle length is more than twice the kMT length. This implies that a tension-sensitive, Ipl1p-dependent error correction mechanism would continuously promote detachment and recapture of kMTs regardless of attachment status until the spindle is ≥1 μm long (Figure 5A). A priori, such repeated rounds of random detachment and reattachment would isomerize the attachment geometry, resulting in spindles with an equal probability for each of the 32 kinetochores to get linked to either of the two SPBs (50% bioriented and 50% syntelic divided equally among the two SPBs). Consistent with this hypothesis, for WT spindles ~1.2 μm in length, we observed a 50%:50% split between unseparated (syntelic) and separated (bioriented) CEN IV tags (Figure 1L) and a symmetric distribution of Ndc80-GFP intensity into two lobes (Figure S1B). In this model, Ipl1p is essential for the isomerization of attachments (Figure 5B). In agreement with this, *ipl1-321* cells displayed highly asymmetric Ndc80-GFP intensity distributions (Figures 2A and 2B), and nearly 100% of the ~1 μm spindles contained unseparated tags (Figure 2E). Remarkably, these cells also maintained SPB−CEN distances at ~0.4 μm (Table S2 and Figures 2C and 5B), showing that Ipl1p is not critically implicated in microtubule length control.

Given that kMT lengths are regulated at ~400 nm, sisters with bipolar attachment begin to sense tension in spindles that are >1 μm in length. It is well established that, in this configuration, each of the sister kinetochores pulls centromere-flanking DNA into a C loop while the sister-chromatid arms remain paired by cohesion (Pearson et al., 2001; Yeh et al., 2008). As a result of spindle elongation, sister kinetochores are no longer exposed to Ipl1p activity, which remains associated with the cohesive portion of the chromatin (Tanaka et al., 2002). Bioriented sisters therefore have more stable attachments than syntelic attachments, which continue to isomerize in a stochastic process under the influence of Ipl1p. Consistent with the notion of a purely random syntely resolution without the need for any decision making by "smart kinetochores" (Indjeian and Murray, 2007), the fraction of unseparated CEN IV tags decreased over time in an exponential decay curve with first-order kinetics (Figure 1L). After converting spindle elongation as the scale of mitotic progression into time (Supplemental Information), we found that the characteristic time for the resolution of one syntelic attachment is ~800 s (Figure S5A). This timescale increased by one order of magnitude to ~8,000 s in *ipl1-321*strains (Figure S5B), indicating that Ipl1p plays a prominent role during all of mitotic progression. In this model, deregulation of the SPB-CEN distance, as we observed in *cin8Δ* strains, would be expected to compromise the discrimination between bioriented and syntelic chromatids. Indeed, whereas *cin8Δ* alone has a fairly mild phenotype, the synthetic lethality of *cin8Δ* with deletion of the checkpoint component *MAD2* (Geiser et al., 1997) supports such a defect.

Implications for Recapture of Monotelic Attachments

Our model implies that, the later syntely is corrected, the longer the MTs must be that project from an SPB to the more distant kinetochore lobe. Consistent with this idea, our data show that establishment of spindle bipolarity is substantially compromised in *stu2-277* mutants, which have fewer long microtubules than

(G) Kymograph aligned with respect to the position of SPB A of a *cin8Δ* cell entering anaphase at time ~80 s. At T = 60 s, the CEN IV tags separate, but both cross the spindle midzone and then fuse again and cross back on the other side (time = 76 s), before they separate permanently.
(H) Histograms of SPB-CEN distances in cells with unseparated tags (blue) and separated tags (red) (analogous to Figure 1H for WT cells).
(I and J) Raw (I) and normalized (J) distributions of spindle lengths and their classification into spindles with unseparated (blue), separated (light red), and reclassified as separated (dark red) CEN IV tags. White solid and dashed lines indicate mean ± bootstrapped SD of cells with syntely (see Figures 1J and 1L). See also Tables S1 and S2 and Movie S7.

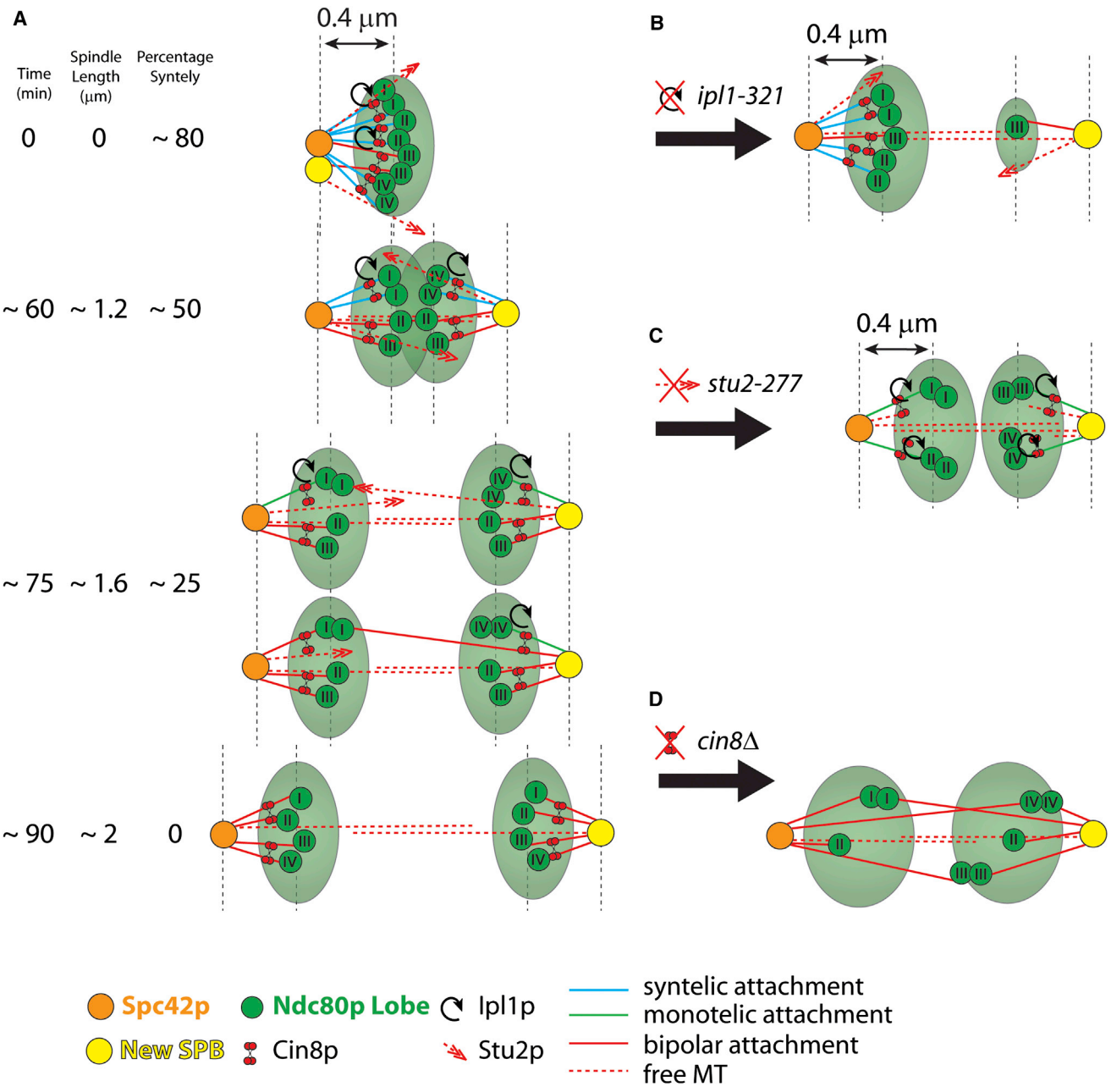

Figure 5. Model for Mitosis Progression and Bipolarity Establishment in Budding Yeast

(A) Schematic mitotic progression (from top to bottom) and bipolarity establishment in WT budding yeast cells.

(B) Model changes in *ipl1-321* cells. Cells have a large percentage of syntelic attachments to one SPB and, as a result, have an asymmetric Ndc80p distribution.

(C) Model changes in *stu2-277* cells. Cells have equal numbers of attachments to both SPBs but have a substantial fraction of monotelic attachments. The overall Ndc80p distribution is bilobed.

(D) Model changes in *cin8Δ* cells. Cells establish bipolar attachments but do not constrain kinetochore microtubule lengths. This results in wider Ndc80p bilobes and frequent crossings of the spindle midzone by centromere tags.

See also Figure S5.

WT cells (Figure 5C). We also found that the ratio between kMTs and interpolar microtubules is much lower in *stu2-277* than in WT cells (Figure S4B), suggesting that a significant number of the mono-oriented attachments are not syntelic but monotelic. We surmise that *STU2* mutations lower the probability for formation and capture of long kMTs from the distant pole and for binding to kMTs from the proximal pole. Consistent with this proposal, we and others have noted an increase in the number of detached sister pairs in *stu2-277* cells; the kinetochores on these detached chromosomes (but curiously not those lying within the

kinetochore lobes) bind Mad2p and provoke checkpoint-dependent mitotic arrest (Gillett et al., 2004). Based on our data, it seems that kMTs are unable to reach across the spindle midzone and capture distant kinetochores, leaving most chromatid pairs mono-oriented.

Implications for Spindle Organization

Our model predicts that kMTs must transiently project from one SPB across the spindle midzone to the kinetochore cluster near the opposite SPB. We know that there cannot be too many of these kMTs at any one time because electron microscopy (EM) reveals very few microtubules at the midzone beyond the two sets of four that run from pole to pole (Winey et al., 1995). However, given the fast MT turnover relative to the size of the nucleus (Table S2), long "projecting" MTs do not last for more than a few seconds and are unlikely to be captured by the EM snapshot of the MT configuration. The model also suggests an alternative explanation for the observed recovery of kinetochore protein fluorescence following photobleaching of one of the two lobes (Pearson et al., 2004). This was originally interpreted as reflecting midzone crossing by kinetochores having bipolar attachments, but we propose that it actually arises when kinetochores transition from syntelic to bipolar attachment and thus one of them changes spindle side. Indeed, predicted recovery rates based on our direct analysis of syntely resolution agree quantitatively with the measurements of fluorescent recovery after photobleaching (FRAP) published by Pearson et al. (2004) (see Extended Experimental Procedures and Figure S3J).

Our model further predicts that the lower rates of FRAP observed in *STU2* mutant cells (Kosco et al., 2001) do not originate from lower kMT dynamics but instead originate from the lack of the long projecting microtubules necessary to convert monopolar to bipolar attachments. Consistent with this, measurements of chromosomal directional instability show very similar switching between growth and shrinkage and vice versa for WT and *stu2-277* cells (Table S2). Hence, loss of function of Stu2p does not primarily affect the dynamics of attached kMTs but specifically lowers the efficiency of growth of unattached spindle MTs.

Relation between Kinetochore Attachment and Aneuploidy

Cancer cells characterized by persistent aneuploidy have hyperstable kinetochore-kMT attachments (Bakhoum et al., 2009). Our model provides a possible explanation for this curious behavior, as it demonstrates that the resolution of syntely is sensitive to the rate of kinetochore detachment. Studies of tetraploid cells in yeast (Mayer and Aguilera, 1990; Storchová et al., 2006) and mice (Fujiwara et al., 2005) have shown that increases in ploidy compromise the fidelity of chromosome segregation. Our model offers a possible explanation also for this observation. The greater the number of chromosomes in a cell, the greater the number of syntelic attachments and the longer it takes to convert them into bipolar attachments. This increase in the time required for bipolarity establishment, accompanied by gradual adaptation of the spindle checkpoint (Rudner and Murray, 1996), would result in increased rates of missegregation. Thus, the current analysis of mitotic progression and chromosome biorientation in yeast unifies our understanding of mitosis in simple and complex eukaryotes and suggests several testable hypotheses about the origins of chromosome missegregation and aneuploidy in general.

EXPERIMENTAL PROCEDURES

Yeast Strains and Growth Conditions

Yeast strains were grown and prepared for microscopy using standard conditions (Rines et al., 2004). See Extended Experimental Procedures for details.

Microscopy

All images were acquired using DeltaVision microscopes (Applied Precision Inc.) with 100× lenses and a Photometrics CoolSnap HQ camera. See Extended Experimental Procedures for details.

Image and Data Analysis

Kinetochore-Snapshot Assay

Our goal was to measure and visualize the distribution of kinetochores along the spindle as a function of spindle length. An analogous procedure was followed to analyze tubulin. In general terms, we detected SPBs and extracted Ndc80-GFP or Tub1-GFP intensities as in Sprague et al. (2003). However, intensities were extracted from 3D stacks to capture all of the signal (see Extended Experimental Procedures). We visualized the distribution of kinetochores or tubulin as a function of spindle length using V plots, in which the fluorescence for a given spindle length is plotted along a horizontal strip, with color encoding the intensity (see Extended Experimental Procedures).

CEN IV-Tracking Assay

Our goal was to track the dynamic behavior of an individual chromosome for 100–300 s in mitosis. SPBs and CEN IV tag positions were determined in 3D using a modified version of the super-resolution spot detection approach in Dorn et al. (2005), allowing us to quantify the dynamics of chromosomal directional instability (see Extended Experimental Procedures). We considered that a CEN crossed the midzone if it was observed for at least five frames on each side of the spindle equator, defined as the middle 20% of the spindle length.

CEN IV-Snapshot Assay

To map out the progression of establishing bipolar attachments, we detected the presence or absence of sister separation in chromosome IV in large cell populations and related the state to the SPB-SPB distances, which served as a surrogate for mitotic progression. To measure separation of CEN IV tags, as well as SPB-CEN distances, it was critical to use super-resolution methods (see Extended Experimental Procedures). We applied the algorithm described in Thomann et al. (2002) to separate overlapping point spread functions. Because the resolution gain by this method increases with a higher signal-to-noise ratio, we imaged snapshots of many spindles at one time point with higher exposure times for additional photon collection. Tension across bioriented sisters sometimes unraveled the Tet-operator sequence in one of the two sisters, which would cause misclassifications of sisters as still unseparated. To correct such errors, we developed an algorithm for reclassification of configurations with only three detectable spots based on the relative intensities between CEN and SPB tags (see Extended Experimental Procedures).

SUPPLEMENTAL INFORMATION

Supplemental Information includes Extended Experimental Procedures, five figures, two tables, and seven movies and can be found with this article online at http://dx.doi.org/10.1016/j.cell.2013.08.008.

ACKNOWLEDGMENTS

We thank T. Warsi, E. Gillett, M.C. Hou, M. Niepel, S. Ventz, A.W. Murray, D. Needleman, and L. Serrano for discussions. E.M. gratefully acknowledges Guo-Cheng Yuan for his encouragement. This work was funded by the grant NIH R01 GM068956 to P.K.S. and G.D. E.M. was supported in part by a long-term fellowship from the Human Frontier Science Program.

Received: November 21, 2012
Revised: May 1, 2013
Accepted: August 7, 2013
Published: August 29, 2013

REFERENCES

Bakhoum, S.F., Genovese, G., and Compton, D.A. (2009). Deviant kinetochore microtubule dynamics underlie chromosomal instability. Curr. Biol. *19*, 1937–1942.

Biggins, S., Severin, F.F., Bhalla, N., Sassoon, I., Hyman, A.A., and Murray, A.W. (1999). The conserved protein kinase Ipl1 regulates microtubule binding to kinetochores in budding yeast. Genes Dev. *13*, 532–544.

Brouhard, G.J., Stear, J.H., Noetzel, T.L., Al-Bassam, J., Kinoshita, K., Harrison, S.C., Howard, J., and Hyman, A.A. (2008). XMAP215 is a processive microtubule polymerase. Cell *132*, 79–88.

Chan, C.S., and Botstein, D. (1993). Isolation and characterization of chromosome-gain and increase-in-ploidy mutants in yeast. Genetics *135*, 677–691.

Chandhok, N.S., and Pellman, D. (2009). A little CIN may cost a lot: revisiting aneuploidy and cancer. Curr. Opin. Genet. Dev. *19*, 74–81.

Cimini, D., Wan, X., Hirel, C.B., and Salmon, E.D. (2006). Aurora kinase promotes turnover of kinetochore microtubules to reduce chromosome segregation errors. Curr. Biol. *16*, 1711–1718.

Dorn, J.F., Jaqaman, K., Rines, D.R., Jelson, G.S., Sorger, P.K., and Danuser, G. (2005). Yeast kinetochore microtubule dynamics analyzed by high-resolution three-dimensional microscopy. Biophys. J. *89*, 2835–2854.

Draviam, V.M., Xie, S., and Sorger, P.K. (2004). Chromosome segregation and genomic stability. Curr. Opin. Genet. Dev. *14*, 120–125.

Fujiwara, T., Bandi, M., Nitta, M., Ivanova, E.V., Bronson, R.T., and Pellman, D. (2005). Cytokinesis failure generating tetraploids promotes tumorigenesis in p53-null cells. Nature *437*, 1043–1047.

Gardner, M.K., Pearson, C.G., Sprague, B.L., Zarzar, T.R., Bloom, K., Salmon, E.D., and Odde, D.J. (2005). Tension-dependent regulation of microtubule dynamics at kinetochores can explain metaphase congression in yeast. Mol. Biol. Cell *16*, 3764–3775.

Gardner, M.K., Bouck, D.C., Paliulis, L.V., Meehl, J.B., O'Toole, E.T., Haase, J., Soubry, A., Joglekar, A.P., Winey, M., Salmon, E.D., et al. (2008). Chromosome congression by Kinesin-5 motor-mediated disassembly of longer kinetochore microtubules. Cell *135*, 894–906.

Geiser, J.R., Schott, E.J., Kingsbury, T.J., Cole, N.B., Totis, L.J., Bhattacharyya, G., He, L., and Hoyt, M.A. (1997). Saccharomyces cerevisiae genes required in the absence of the CIN8-encoded spindle motor act in functionally diverse mitotic pathways. Mol. Biol. Cell *8*, 1035–1050.

Gillett, E.S., Espelin, C.W., and Sorger, P.K. (2004). Spindle checkpoint proteins and chromosome-microtubule attachment in budding yeast. J. Cell Biol. *164*, 535–546.

Goshima, G., and Yanagida, M. (2000). Establishing biorientation occurs with precocious separation of the sister kinetochores, but not the arms, in the early spindle of budding yeast. Cell *100*, 619–633.

He, X., Asthana, S., and Sorger, P.K. (2000). Transient sister chromatid separation and elastic deformation of chromosomes during mitosis in budding yeast. Cell *101*, 763–775.

He, X., Rines, D.R., Espelin, C.W., and Sorger, P.K. (2001). Molecular analysis of kinetochore-microtubule attachment in budding yeast. Cell *106*, 195–206.

Hoyt, M.A., He, L., Loo, K.K., and Saunders, W.S. (1992). Two Saccharomyces cerevisiae kinesin-related gene products required for mitotic spindle assembly. J. Cell Biol. *118*, 109–120.

Hyland, K.M., Kingsbury, J., Koshland, D., and Hieter, P. (1999). Ctf19p: A novel kinetochore protein in Saccharomyces cerevisiae and a potential link between the kinetochore and mitotic spindle. J. Cell Biol. *145*, 15–28.

Indjeian, V.B., and Murray, A.W. (2007). Budding yeast mitotic chromosomes have an intrinsic bias to biorient on the spindle. Curr. Biol. *17*, 1837–1846.

Jaqaman, K., Dorn, J.F., Jelson, G.S., Tytell, J.D., Sorger, P.K., and Danuser, G. (2006). Comparative autoregressive moving average analysis of kinetochore microtubule dynamics in yeast. Biophys. J. *91*, 2312–2325.

Jaspersen, S.L., and Winey, M. (2004). The budding yeast spindle pole body: structure, duplication, and function. Annu. Rev. Cell Dev. Biol. *20*, 1–28.

Joglekar, A.P., Bloom, K., and Salmon, E.D. (2009). In vivo protein architecture of the eukaryotic kinetochore with nanometer scale accuracy. Curr. Biol. *19*, 694–699.

Kim, J.H., Kang, J.S., and Chan, C.S. (1999). Sli15 associates with the ipl1 protein kinase to promote proper chromosome segregation in Saccharomyces cerevisiae. J. Cell Biol. *145*, 1381–1394.

Kitagawa, K., and Hieter, P. (2001). Evolutionary conservation between budding yeast and human kinetochores. Nat. Rev. Mol. Cell Biol. *2*, 678–687.

Knowlton, A.L., Lan, W., and Stukenberg, P.T. (2006). Aurora B is enriched at merotelic attachment sites, where it regulates MCAK. Curr. Biol. *16*, 1705–1710.

Kosco, K.A., Pearson, C.G., Maddox, P.S., Wang, P.J., Adams, I.R., Salmon, E.D., Bloom, K., and Huffaker, T.C. (2001). Control of microtubule dynamics by Stu2p is essential for spindle orientation and metaphase chromosome alignment in yeast. Mol. Biol. Cell *12*, 2870–2880.

Maure, J.F., Kitamura, E., and Tanaka, T.U. (2007). Mps1 kinase promotes sister-kinetochore bi-orientation by a tension-dependent mechanism. Curr. Biol. *17*, 2175–2182.

Mayer, V.W., and Aguilera, A. (1990). High levels of chromosome instability in polyploids of Saccharomyces cerevisiae. Mutat. Res. *231*, 177–186.

Meyer, R.E., Kim, S., Obeso, D., Straight, P.D., Winey, M., and Dawson, D.S. (2013). Mps1 and Ipl1/Aurora B act sequentially to correctly orient chromosomes on the meiotic spindle of budding yeast. Science *339*, 1071–1074.

O'Toole, E.T., Winey, M., and McIntosh, J.R. (1999). High-voltage electron tomography of spindle pole bodies and early mitotic spindles in the yeast Saccharomyces cerevisiae. Mol. Biol. Cell *10*, 2017–2031.

Pearson, C.G., Maddox, P.S., Salmon, E.D., and Bloom, K. (2001). Budding yeast chromosome structure and dynamics during mitosis. J. Cell Biol. *152*, 1255–1266.

Pearson, C.G., Maddox, P.S., Zarzar, T.R., Salmon, E.D., and Bloom, K. (2003). Yeast kinetochores do not stabilize Stu2p-dependent spindle microtubule dynamics. Mol. Biol. Cell *14*, 4181–4195.

Pearson, C.G., Yeh, E., Gardner, M., Odde, D., Salmon, E.D., and Bloom, K. (2004). Stable kinetochore-microtubule attachment constrains centromere positioning in metaphase. Curr. Biol. *14*, 1962–1967.

Pinsky, B.A., and Biggins, S. (2005). The spindle checkpoint: tension versus attachment. Trends Cell Biol. *15*, 486–493.

Pinsky, B.A., Tatsutani, S.Y., Collins, K.A., and Biggins, S. (2003). An Mtw1 complex promotes kinetochore biorientation that is monitored by the Ipl1/Aurora protein kinase. Dev. Cell *5*, 735–745.

Rines, D., Thomann, D., Dorn, J., Goodwin, P., and Sorger, P.K. (2004). Live cell imaging of yeast. In Live Cell Imaging: A Laboratory Manual, R.D. Goldman and D.L. Spector, eds. (Woodbury, NY: Cold Spring Harbor Laboratory Press), p. 631.

Rudner, A.D., and Murray, A.W. (1996). The spindle assembly checkpoint. Curr. Opin. Cell Biol. *8*, 773–780.

Severin, F., Habermann, B., Huffaker, T., and Hyman, T. (2001). Stu2 promotes mitotic spindle elongation in anaphase. J. Cell Biol. *153*, 435–442.

Sprague, B.L., Pearson, C.G., Maddox, P.S., Bloom, K.S., Salmon, E.D., and Odde, D.J. (2003). Mechanisms of microtubule-based kinetochore positioning in the yeast metaphase spindle. Biophys. J. *84*, 3529–3546.

Storchová, Z., Breneman, A., Cande, J., Dunn, J., Burbank, K., O'Toole, E., and Pellman, D. (2006). Genome-wide genetic analysis of polyploidy in yeast. Nature *443*, 541–547.

Su, X., Qiu, W., Gupta, M.L., Jr., Pereira-Leal, J.B., Reck-Peterson, S.L., and Pellman, D. (2011). Mechanisms underlying the dual-mode regulation of microtubule dynamics by Kip3/kinesin-8. Mol. Cell *43*, 751–763.

Tanaka, T.U., Rachidi, N., Janke, C., Pereira, G., Galova, M., Schiebel, E., Stark, M.J., and Nasmyth, K. (2002). Evidence that the Ipl1-Sli15 (Aurora kinase-INCENP) complex promotes chromosome bi-orientation by altering kinetochore-spindle pole connections. Cell *108*, 317–329.

Thomann, D., Rines, D.R., Sorger, P.K., and Danuser, G. (2002). Automatic fluorescent tag detection in 3D with super-resolution: application to the analysis of chromosome movement. J. Microsc. *208*, 49–64.

Thomann, D., Dorn, J., Sorger, P.K., and Danuser, G. (2003). Automatic fluorescent tag localization II: Improvement in super-resolution by relative tracking. J. Microsc. *211*, 230–248.

Thompson, S.L., Bakhoum, S.F., and Compton, D.A. (2010). Mechanisms of chromosomal instability. Curr. Biol. *20*, R285–R295.

Tytell, J.D., and Sorger, P.K. (2006). Analysis of kinesin motor function at budding yeast kinetochores. J. Cell Biol. *172*, 861–874.

Varga, V., Leduc, C., Bormuth, V., Diez, S., and Howard, J. (2009). Kinesin-8 motors act cooperatively to mediate length-dependent microtubule depolymerization. Cell *138*, 1174–1183.

Vasquez, R.J., Gard, D.L., and Cassimeris, L. (1994). XMAP from Xenopus eggs promotes rapid plus end assembly of microtubules and rapid microtubule polymer turnover. J. Cell Biol. *127*, 985–993.

Wang, P.J., and Huffaker, T.C. (1997). Stu2p: A microtubule-binding protein that is an essential component of the yeast spindle pole body. J. Cell Biol. *139*, 1271–1280.

Winey, M., Mamay, C.L., O'Toole, E.T., Mastronarde, D.N., Giddings, T.H., Jr., McDonald, K.L., and McIntosh, J.R. (1995). Three-dimensional ultrastructural analysis of the Saccharomyces cerevisiae mitotic spindle. J. Cell Biol. *129*, 1601–1615.

Yeh, E., Haase, J., Paliulis, L.V., Joglekar, A., Bond, L., Bouck, D., Salmon, E.D., and Bloom, K.S. (2008). Pericentric chromatin is organized into an intramolecular loop in mitosis. Curr. Biol. *18*, 81–90.

Zeng, X., Kahana, J.A., Silver, P.A., Morphew, M.K., McIntosh, J.R., Fitch, I.T., Carbon, J., and Saunders, W.S. (1999). Slk19p is a centromere protein that functions to stabilize mitotic spindles. J. Cell Biol. *146*, 415–425.